ORIGINAL ARTICLE

Korean J Intern Med 2022;37:411-424
https://doi.org/10.3904/kjim.2020.438

Alleviation of renal ischemia/reperfusion injury by exosomes from induced pluripotent stem cell-derived mesenchymal stem cells

Sun Woo Lim[1,2,*], Kyung Woon Kim[2,3,*], Bo Mi Kim[2], Yoo Jin Shin[1,2], Kang Luo[1,2], Yi Quan[1,2], Sheng Cui[1,2], Eun Jeong Ko[1,2,4], Byung Ha Chung[1,2,4], and Chul Woo Yang[1,2,4]

[1]Transplant Research Center, College of Medicine, The Catholic University of Korea, Seoul; [2]Convergent Research Consortium for Immunologic Disease, Seoul St. Mary's Hospital, College of Medicine, The Catholic University of Korea, Seoul; [3]R&D Center, OncoInsight Co. Ltd., Seoul; [4]Division of Nephrology, Department of Internal Medicine, Seoul St. Mary's Hospital, College of Medicine, The Catholic University of Korea, Seoul, Korea

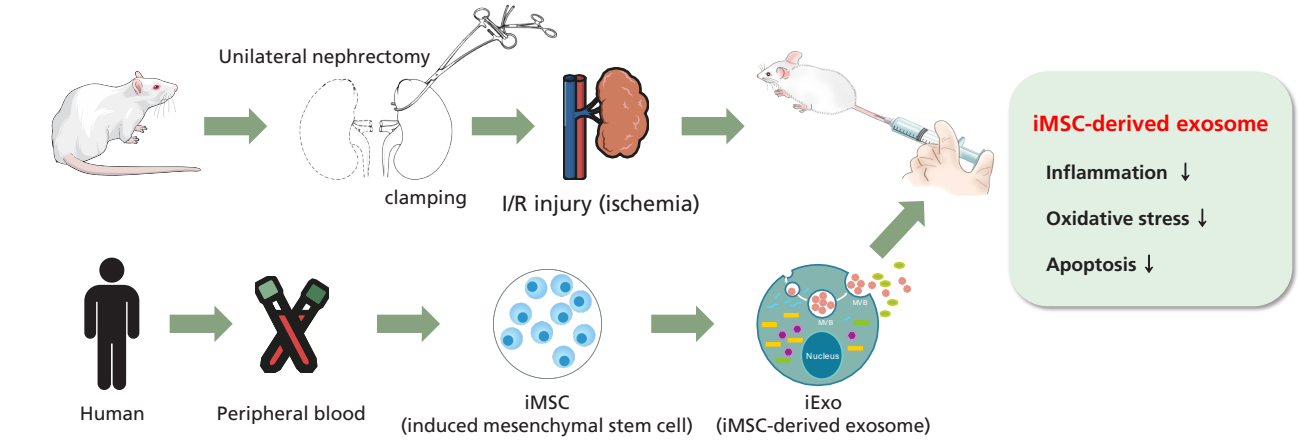

Conclusion

iMSC-derived exosomes may provide a novel therapeutic approach for AKI treatment.

Received : August 19, 2020
Revised : November 18, 2020
Accepted : November 20, 2020

Correspondence to Chul Woo Yang, M.D.
Division of Nephrology, Department of Internal Medicine, Seoul St. Mary's Hospital, College of Medicine, The Catholic University of Korea, 222 Banpo-daero, Seocho-gu, Seoul 06591, Korea
Tel: +82-2-2258-6851, Fax: +82-2-2258-6917, E-mail: yangch@catholic.ac.kr
https://orcid.org/0000-0001-9796-636X

*These authors contributed equally to this work.

pISSN 1226-3303
eISSN 2005-6648
http://www.kjim.org

Background/Aims: Renal ischemia followed by reperfusion (I/R) is a leading cause of acute kidney injury (AKI), which is closely associated with high morbidity and mortality. Studies have shown that induced pluripotent stem cell (iPSC)-derived mesenchymal stem cells (iMSCs) exert powerful therapeutic effects in renal ischemia. However, the efficacy of iMSC-derived exosomes (iExo) on I/R injuries remains largely unknown.
Methods: Human iPSCs were differentiated into iMSCs using a modified one-step method. Ultrafiltration, combined with purification, was used to isolate iExo from iMSCs. iExo was administered following I/R injury in a mouse model. The effect of iExo on I/R injury was assessed through changes in renal function, histology, and expression of oxidative stress, inflammation, and apoptosis markers. Further, we evaluated its association with the extracellular signal-regulated kinase (ERK) 1/2 signaling pathway.
Results: Mice subjected to I/R injury exhibited typical AKI patterns; serum creatinine level, tubular necrosis, apoptosis, inflammatory cytokine production, and oxidative stress were markedly increased compared to sham mice. However, treatment with iExo attenuated these changes, significantly improving renal function and tissue damage, similar to the renoprotective effects of iMSCs on I/R injury. Significant induction of activated ERK 1/2 signaling molecules was observed in mice treated with iExo compared to those in the I/R injury group.
Conclusions: The present study demonstrates that iExo administration ameliorated renal damage following I/R, suggesting that iMSC-derived exosomes may provide a novel therapeutic approach for AKI treatment.

Keywords: Acute kidney injury; Reperfusion injury; Induced pluripotent stem cell; Mesenchymal stem cell; Exosomes

INTRODUCTION

Renal ischemia followed by ischemia reperfusion (I/R) is a leading cause of acute kidney injury (AKI) and acute kidney failure, which are associated with high morbidity and mortality. Previous studies have shown that ischemia is related to epithelial cell necrosis and endothelial cell dysfunction; reperfusion can also result in renal tubular cell apoptosis [1-4]. Acute tubular necrosis induced by I/R injury severely affects kidney graft outcomes in transplanted kidneys [3,5-7]. Therefore, I/R injury is a critical clinical challenge in both native and transplanted kidneys, with limited effective treatments available.

Recent advances in stem cell technology have enabled the generation of patient-specific induced pluripotent stem cells (iPSCs) from adult somatic cells, which can differentiate into expandable progenitor cells and mature cells [8]. iPSCs exhibit similar properties with embryonic stem cells (ESCs) with self-renewal and differentiation properties. However, one distinct advantage over ESCs is that iPSCs are patient-specific and, therefore, theoretically, can overcome the need for immunosuppression in the recipient. iPSCs can generate unlimited amounts of early passage patient-specific mesenchymal stem cells (MSCs) with consistent quality. iPSC-derived MSCs (iMSCs) provide a promising cell source for autologous cell therapies in regenerative medicine because of their more powerful therapeutic function compared to bone marrow-derived mesenchymal stem/stromal cells (BMSCs) [9,10].

Although it has been demonstrated that MSCs exhibit advantages in cell therapy, one potential challenge is their acquisition of genetic and epigenetic alterations. MSCs become immortalized after long-term culture and can spontaneously transform into malignant cells due to enhanced chromosomal instability associated with dysregulation of telomere activity and cell cycle-related genes, resulting in tumorigenesis when injected into multiple organs [11]. Jeong et al. [12] found that even short-term cultured MSCs transplanted into mice can transform into malignant tumors. Therefore, determining how to fully advantageously use MSCs while avoiding the adverse effects, such as tumor formation, is an important step toward their application in the clinical setting. Recently, accumulating evidence has indicated that the therapeutic action of stem cells is mainly exerted through the secretion of molecules such as growth factors, cytokines, chemokines, and extracellular microvesicles into the surrounding environment via a paracrine mechanism [13]. Among these paracrine molecules, exosomes demonstrate unique functions in disease diagnosis and therapy [14,15]. Exosomes are small membrane vesicles (40 to 100

https://doi.org/10.3904/kjim.2020.438

nm diameter) of endosomal origin formed in multivesicular bodies (MVBs) by invagination of the endosomal membrane and then released into the extracellular space when MVBs fuse with the plasma membrane [16].

Recent studies have indicated that exosomes derived from BMSCs can promote angiogenesis in ischemic tissue and attenuate tissue damage after ischemic injury [17-19]. Further, it has been confirmed that exosomes derived from MSCs are immune-tolerant, an important property for clinical applications [20]. Therefore, we hypothesized that exosomes derived from iMSCs (iExo) may similarly reduce tissue injury after I/R. In the present study, we investigated the therapeutic effect of iExo in a mouse renal I/R model, demonstrating important implications for new therapeutic approaches to AKI.

METHODS

Generation of human iPSCs from peripheral blood mononuclear cells

Peripheral blood samples were obtained from healthy human donors after obtaining informed consent, with approval of the Institutional Review Board of Seoul St. Mary's Hospital (KIRB-00613_6-001). Peripheral blood mononuclear cells (PBMCs) were isolated via centrifugation using Ficoll-Paque PLUS media (GE Healthcare Bio-Sciences AB, Uppsala, Sweden). Isolated PBMCs were cultured in StemSpan ACF (Stem Cell Technologies, Vancouver, BC, Canada) supplemented with StemSpan CC110 for 4 days. Mononuclear cells were then transferred to a 24-well vitronectin-coated plate (BD BioCoat, BD Biosciences, Franklin Lakes, NJ, USA), and Sendai virus (SeV) (CytoTune-iPSC 2.0 Reprogramming kit, Thermo Fisher Scientific, Waltham, MA, USA) was added to give a multiplicity of infection of three (MOI:3). The medium was changed daily until iPSC colonies formed. After manual picking, iPSC lines were maintained on vitronectin-coated plates (Thermo Fisher Scientific) in a TeSR-E8 medium (Stem Cell Technologies). Emerging iPSC colonies were picked individually and expanded for characterization on day 12 after transduction. Cells were cultured in a 37°C incubator with 5% CO_2 from days 3 to 21 after transduction.

Generation of MSCs from iPSCs

To reprogram iPSCs into iMSCs, iPSCs were dissociated with the aid of Versene thylene-diamine-tetraacetic acid (Thermo Fisher Scientific) and seeded into nonadherent 6-well conical polymerase chain reaction plates (10,000 cells per well) with Iscove's Modified Dulbecco's Medium (MDM basal media, 17% KnockOut Serum Replacement, 1% minimal essential medium nonessential amino acids, 110 mM 2-mercaptoethanol, and 1% PSA antifungal-antibacterial solution; Thermo Fisher Scientific). On day 2, embryoid bodies (EBs) were transferred to nonadherent 2.4 mg/cm^2 poly-HEMA-coated flasks and cultured for 3 more days. On day 5, EBs were transferred to 1% gelatin-treated flasks for 3 more days. On day 8, some EBs were attached to the surface and cells grew outward from the EBs. Non-attached EBs were transferred to another 1% gelatin-coated flask. Cells were fed with medium supplemented with 10 ng/mL TGF-β1 (R&D Systems, Minneapolis, MN, USA) on days 8 to 10, after which the medium was switched to standard Dulbecco's Modified Eagle Medium culture medium containing 10% fetal bovine serum, 2 mM L-glutamine, and 100 U/mL penicillin/streptomycin (Thermo Fisher Scientific). The medium was changed twice weekly, and cells were split upon confluence in a 1:3 ratio. The same iMSC derivation protocol was repeated using three different iPSC control lines.

Isolation and purification of exosomes from iMSC

After iPSC-MSCs reached approximately 80% confluency, the culture medium was replaced with MesenGro hMSC medium (StemRD Inc., Burlingame, CA, USA), and cells were cultured for an additional 48 hours. Conditioned medium (CM) was collected, and exosomes were isolated as previously described [21]. Briefly, the CM was centrifuged sequentially at 300 g for 10 minutes and then at 2,000 g for 10 minutes. Next, cellular debris in CM supernatants was removed via 0.22-μm filtration, and supernatants were ultracentrifuged at 100,000 g for 2 hours. Pelleted exosomes were resuspended in phosphate-buffered saline and then centrifuged at 4,000 g until the volume in the upper compartment was reduced to approximately 200 μL. Total protein concentration in exosomes was quantified using the Micro Bicinchoninic Acid Protein Assay Kit (Thermo Fisher Scientific), according to the manufacturer's recommended protocol. All procedures were performed at 4°C. Exosome morphologies were observed using a JEOL 1200EX transmission electron microscope (TEM; JEOL Ltd., Tokyo, Japan). Primary antibodies against tumor susceptibility gene 101 (TSG101) (Cat#SC-136111, 1:200; Santa Cruz Biotechnol-

ogy, Dallas, TX, USA), CD9 (Cat#SC-13118, 1:200; Santa Cruz Biotechnology), CD63 (Cat#SC-365604, 1:200; Santa Cruz Biotechnology), and secondary antibody were added. Exosomal marker proteins were used to analyze the incorporation of each protein into exosomes in immunoblots.

Flow cytometric analysis

iMSC surface antigens were analyzed using a FACSCalibur flow cytometer (BD Biosciences) employing FlowJo software version 10 (Tree Star, Ashland, OR, USA). The following conjugated monoclonal antibodies (BD Biosciences) were used at concentrations recommended by the manufacturer: CD34-phycoerythrin (PE) (Cat#12-0349-42), CD31-fluorescein isothiocyanate (FITC) (Cat#11-0319-42), CD19-allophycocyanin (APC) (Cat#152409), CD11-FITC (Cat#11-0112-41), human leukocyte antigen–DR isotype (HLA-DR)-FITC (Cat#11-9956-41), CD44-FITC (Cat#11-0441-81), CD73-FITC (Cat#11-0739-41), CD105-FITC (Cat#12-1051-81), and CD90-FITC (Cat#11-0909-41). We also prepared appropriate isotype staining controls.

I/R injury modeling and iMSC or iExo injection

Animal study protocols were approved by the Institutional Animal Care and Use Committee at the Catholic University of Korea (CUMC-2017-0245). AKI was induced by kidney I/R in 8-week-old male BALB/c mice. I/R injury was induced by unilateral renal pedicle clamping plus contralateral nephrectomy, as previously described [22]. After front incisions were made, blood supply to the kidneys was blocked for 25 minutes. Saline, iMSCs (1×10^5 or 2×10^5/mouse), or iExo (10 or 50 or 200 μg/mouse) were injected through the tail vein after reperfusion. Animals were euthanized after 24 hours of reperfusion. Control animals were subjected to sham operations without renal pedicle clamping.

Measurement of serum creatinine

Serum creatinine (sCr) was evaluated by a quantitative enzymatic colorimetric method (0430-120; Stanbio Laboratory, Boerne, TX, USA), according to the manufacturer's instruction.

Histopathological examination

Mouse kidneys were fixed in 4% paraformaldehyde and embedded in paraffin, and 4-um sections were cut and stained with periodic acid-Schiff stain (PAS, Sigma-Aldrich, St. Louis, MO, USA). Renal tubular damage was scored by a blinded renal pathologist. A grade scale of 0 to 5, as outlined by Lien et al. [23], was used for the histopathological assessment of I/R-induced renal injury. Histological changes due to tubular necrosis were quantified by calculating the percentage of tubules displaying acute tubular necrosis (ATN), loss of brush border, cast formation, and tubule dilatation: 0, no damage; 1, < 25% damage; 2, 25% to 50% damage; 3, 50% to 75% damage; 4, 75% to 90% damage; and 5, > 90% damage. At least 10 fields (original magnification ×100) were reviewed in each slide.

In situ terminal deoxynucleotidyl transferase dUTP nick end labeling

Apoptotic cells in mouse kidney tissue sections were detected using the *in situ* terminal deoxynucleotidyl transferase dUTP nick end labeling (TUNEL) method and stained with the *In Situ* Apoptosis Detection Kit (Cat#MER-S7100; MERCK-Millipore, San Diego, CA, USA). TUNEL-positive cells were counted in approximately 20 randomly selected, non-overlapping areas per animal in each group.

Quantitative real-time polymerase chain reaction

Total RNA from mouse kidney tissues was isolated using an RNA-spin Total RNA Extraction Kit (iNtRON Biotechnology Inc., Seongnam, Korea). First-strand cDNA was synthesized using a Reverse Transcription System (Promega, Madison, WI, USA) and subjected to quantitative real-time polymerase chain reaction (qRT-PCR) using SYBR Green Master Mix in the LightCycler 480 system (Roche Life Science, Rotkreuz, Switzerland). Gene expression was normalized to glyceraldehyde 3-phosphate dehydrogenase (GAPDH) expression using the change-in-threshold method and primers with the following sequences: 5′-GGC CAA GGG AGA TGT TAC AAC-3′ and 5′-GCA ACT CTC CTT TGG GTT CTC-3′ for mouse superoxide dismutase 2 (SOD2), 5′-GCG GAT TCC TGA GAG AGT GGT AC-3′ and 5′-GCC TGA CTC TCC AGC GAC TGT GGA G-3′ for mouse catalase, 5′-CAC ATT CCC AAA CAA GAT GC-3′ and 5′-TCT TTT TCC AGC GAG GAG AT-3′ for mouse nuclear factor erythroid-2-related factor (NRF2), 5′-CTT CCT CAG CCA TGG TAC CTC T-3′and 5′-CAA GTC TTC ATC AGC ATC AAA CTG-3′ for mouse nuclear factor κB (NF-κB), 5′-CTT CTC ATT CCT GCT TGT G-3′ and 5′-ACT TGG TGG TTT GCT ACG-3′ for mouse tumor necrosis factor-α (TNFα), 5′-TTC TTC AGC AAC AGC

https://doi.org/10.3904/kjim.2020.438

AAG GC-3′ and 5′-CCT TTT CCT CAG CGA CGA CT-3′ for mouse interferon γ (IFNγ), 5′-TTG TGG CTG TGG AGA AG-3′ and 5′-CAT CAG AGG CAA GGA GG-3′ for mouse interleukin 1β (IL-1β), 5′-CCC ATG TTT GTG ATG GGT GT-3′ and 5′-GTG ATG GCA TGG ACT GTG GT-3′ for mouse GAPDH [22,24].

Detection of 8-OHdG in urine

An enzyme-linked immunosorbent assay (ELISA) kit (Cell Biolabs, San Diego, CA, USA) was used to detect 8-OHdG in spot urine, according to the manufacturer's instructions. Urinary 8-hydroxy-2′-deoxyguanosine (8-OHdG) concentration was calculated as picogram per milligram of creatinine.

Immunohistochemical analysis of 8-OHdG in tissue sections

Immunohistochemistry was carried out as described above [24]. Briefly, 4-μm sections of paraffin-embedded kidney tissue were deparaffinized and then placed in citrate buffer solution (pH 6.0), methanolic H_2O_2, and 0.5% Triton X-100. Nonspecific binding sites were blocked in 10% normal donkey serum (Jackson ImmunoResearch, West Grove, PA, USA). Sections were incubated overnight at 4°C with anti-8-OHdG antibodies (Cat#MOG-100P, JaICA, Shizuoka, Japan) and then with peroxidase-conjugated secondary antibodies for 2 hours at room temperature. Peroxidase activity was detected using 3,3′-diaminobenzidine (Vector Laboratories, Burlingame, CA, USA) as a chromogen. Quantitative analysis was performed by calculating the 8-OHdG positive area showing the same intensity, using histogram equalization (TDI Scope Eye version 3.6 for Windows, JN OpTIC, Seoul, Korea).

Immunoblot analysis

Whole kidneys were lysed in 10 mM Tris (pH 7.5) containing 1% sodium dodecyl sulfate and 1 mM $NaVO_4$. Equal amounts of protein were subjected to immunoblot analysis using the following primary antibodies from Cell Signaling Technology: phosphorylated-mitogen-activated protein kinase kinase 1/2 (p-MEK1/2; Cat#9121), total-MEK1/2 (Cat#8727), p-EKR1/2 (Cat#9101), and total-ERK1/2 (Cat#9121). Signals were detected using an enhanced chemiluminescence system (ATTO Corp., Tokyo, Japan). Quantification of relative intensities was performed with the sham group set as 100%; densities were normalized to that of total form bands from the same gel using Quantity One version 4.4.0 software (Bio-Rad Laboratories, Hercules, CA, USA).

Statistical analyses

Data were expressed as the mean ± standard error from at least three independent experiments. Multiple comparisons between groups were performed via a one-way analysis of variance with Bonferroni post hoc testing using Prism software version 7.03 for Windows (GraphPad Software, La Jolla, CA, USA). Results with p values < 0.05 were considered significant.

RESULTS

Characterization of iMSCs and iExo

We successfully derived human MSCs from three different iPSC cell lines using an induction protocol. After culturing in MSC medium for a few days, iPSCs showed a tendency to form packed clones with decreased nuclear:cytoplasmic ratios and formed a monolayer with a larger spindle-shaped morphology at the border of the colonies. After culturing on gelatin-coated dishes for 14 days, cells were continually passaged when they reached 90% confluence until homogeneous fibroblastic morphologies were observed (Fig. 1A). A longitudinal study comparing MSC surface marker expression at passage 5 was conducted using flow cytometry to monitor the transition of iPSCs to the MSC-like phenotype (Fig. 1B). After a few passages in culture, iMSCs expressed similar levels of CD44, CD73, CD105, and CD90 as BMSCs. In TEM experiments with iExo, we observed spheroidal microvesicles that were 30 to 100 nm in diameter (Fig. 1C), indicating the presence of exosomes. Western blot analyses indicated that iExo expressed exosomal markers such as TSG101, CD9, and CD63 proteins (Fig. 1D).

Effects of treatment with iExo or iMSCs on renal function and histology in renal I/R injury mouse model

Mice with I/R injury in the iExo treatment (I/R + iExo) group had significantly lower sCr levels and ATN scores after 24 hours compared to mice in the I/R group, as shown in Fig. 2 (sCr, 1.53 ± 0.31 mg/dL vs. 2.77 ± 0.25 mg/dL; ATN score, 1.3 ± 0.11 vs. 2.3 ± 0.15, $p < 0.05$ vs. the I/R group). Mice treated iMSCs had significantly reduced sCr levels and ATN scores compared to those in the I/R group but did not differ significantly from those in the I/R + iExo group (sCr, 1.35 ± 0.45 mg/dL; ATN score, 1.16 ± 0.09, $p > 0.05$ vs. the I/R + iExo group). The sham groups that received iMSC or iExo

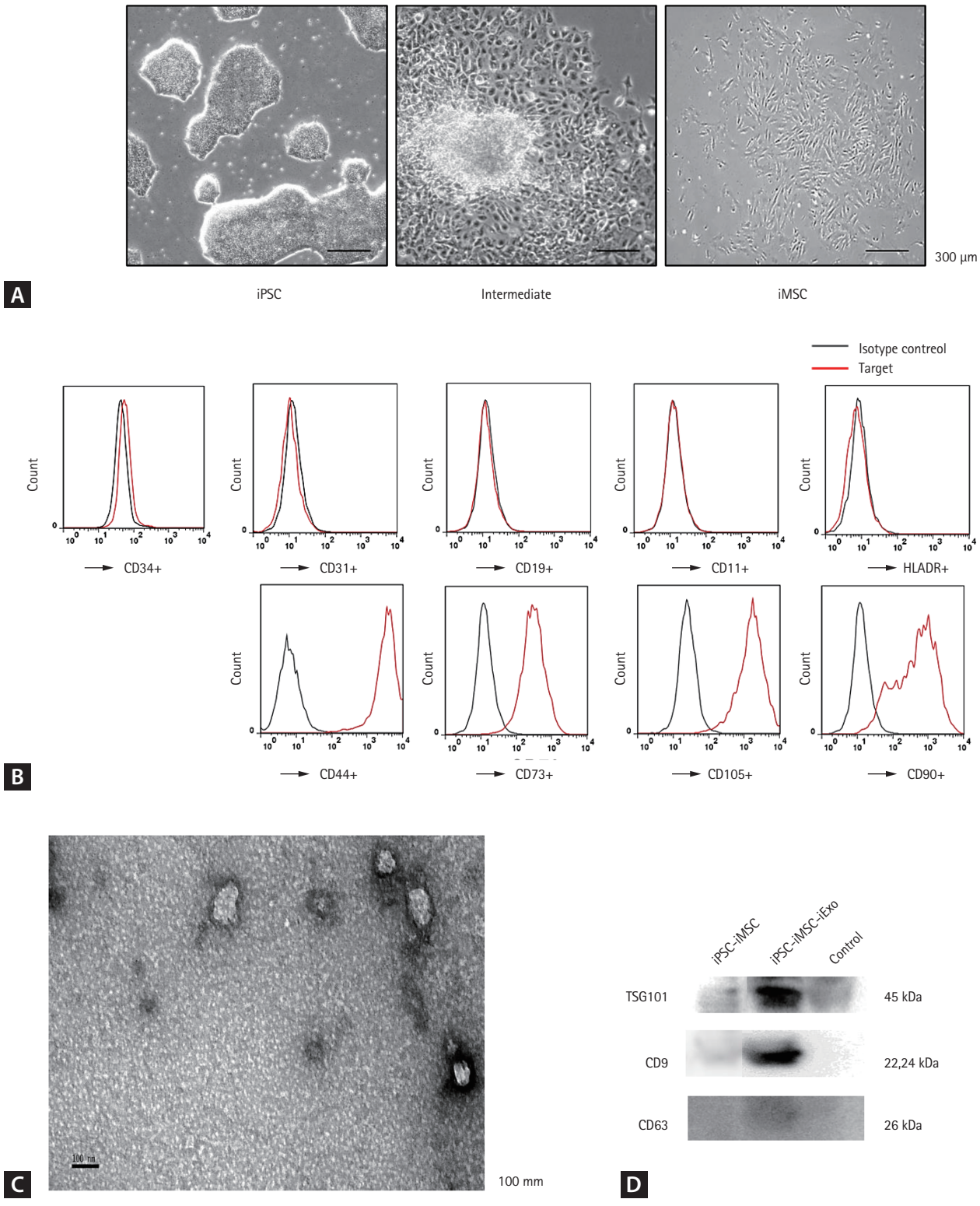

Figure 1. Characterization of induced pluripotent stem cell (iPSC)-derived mesenchymal stem cells (iMSCs) and iMSC-derived exosomes (iExo). (A) Light microscopy images demonstrating morphological changes before iPSC differentiation, during the intermediate phase, and after differentiation into fibroblast-like cells (scale bar = 300 μm). (B) Flow cytometric analysis of mesenchymal-positive markers CD44, CD73, CD105, and CD90, and mesenchymal-negative markers CD34, CD31, CD19, CD11, and human leukocyte antigen–DR isotype (HLA-DR). Black, isotype controls; red, indicated markers. (C) Morphology of iExo under transmission electron microscopy (scale bar = 100 nm). (D) Incorporation of tumor susceptibility gene 101 (TSG101), CD9, and CD63 into iExo detected using immunoblotting.

https://doi.org/10.3904/kjim.2020.438

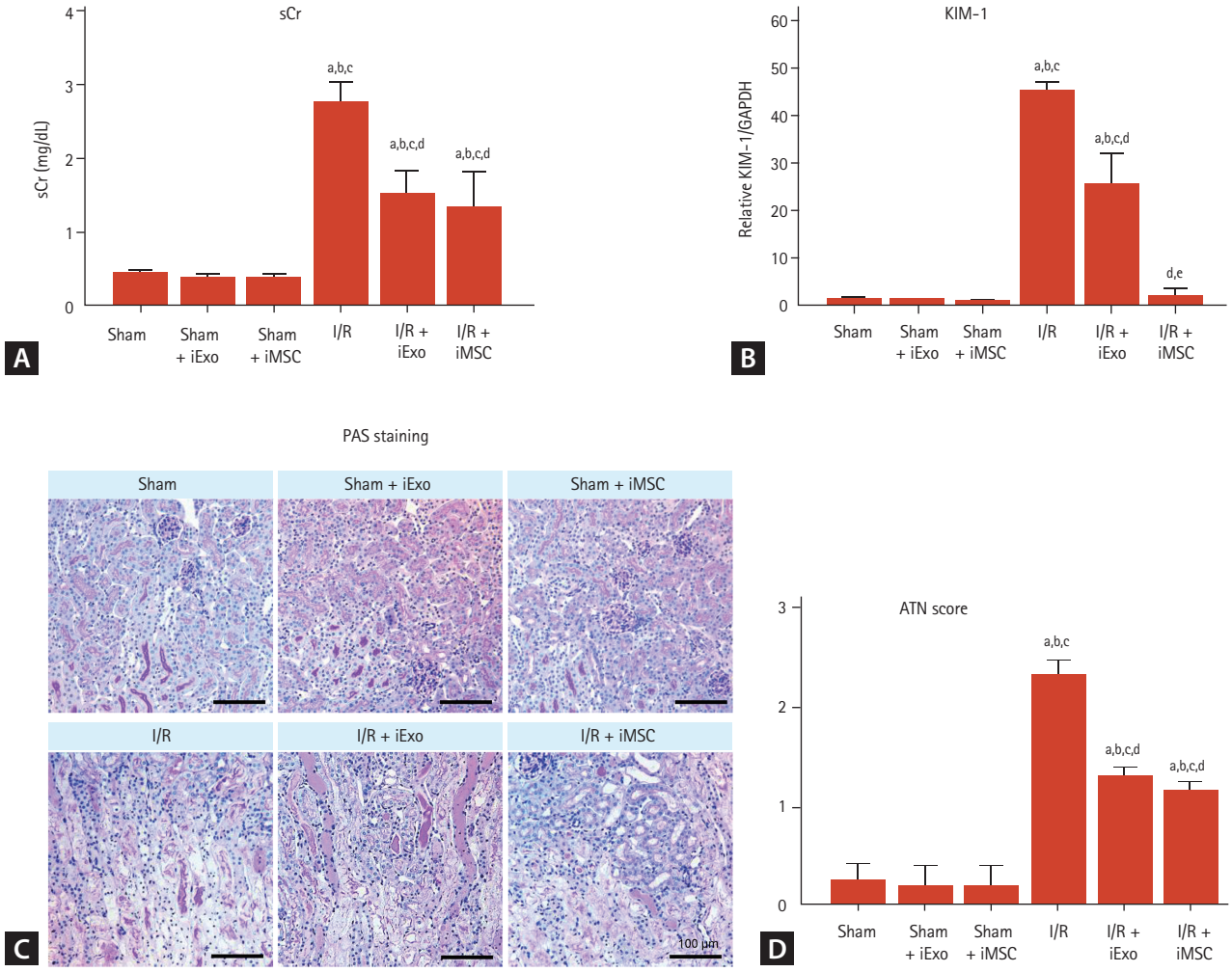

Figure 2. Effects of treatment with mesenchymal stem cells (iMSCs) or iMSC-derived exosome (iExo) on renal function and histology in renal ischemia reperfusion (I/R) injury mouse model. (A) Serum creatinine (sCr) level. (B) Kidney injury marker-1 (KIM-1) mRNA level using quantitative real-time polymerase chain reaction. (C) Representative images of kidney histology from outer stripe of outer medulla. (D) Pathological score of tubular damage. Data are presented as mean ± standard error. Scale bar = 100 μm. GAPDH, glyceraldehyde 3-phosphate dehydrogenase; PAS, periodic acid-Schiff stain; ATN, acute tubular necrosis. [a]$p < 0.05$ vs. Sham, [b]$p < 0.05$ vs. Sham + iMSC, [c]$p < 0.05$ vs. Sham + iExo, [d]$p < 0.05$ vs. I/R, [e]$p < 0.05$ vs. I/R + iExo.

injections did not differ significantly.

Effects of iExo or iMSC treatment on apoptosis induced by renal I/R injury

Next, we investigated whether iMSC or iExo treatment had any effect on the apoptotic process during I/R injury. The sham groups exhibited few TUNEL-positive cells, but treatment with iExo or iMSCs resulted in significantly fewer TUNEL-positive cells (1.8 ± 0.9 and 1.8 ± 0.5 vs. 8.0 ± 0.2, $p < 0.05$ vs. the sham group). In the I/R group, numerous cells were strongly positive for TUNEL staining, as shown in Fig. 3A. In contrast, treatment with iExo and iMSCs resulted in significantly fewer TUNEL-positive cells than the I/R group, although the I/R + iExo and I/R + iMSC groups did not differ significantly (11.6 ± 2.8 and 16.0 ± 3.8 vs. 43.1 ± 8.3, $p < 0.05$ vs. the I/R group) (Fig. 3A and 3B).

Using qRT-PCR analysis, we found that iExo and iMSC treatments reduced mRNA levels of Bim and caspase-3 and restored the B-cell lymphoma 2 (Bcl-2) mRNA level compared to the I/R group (Bim, 1.92 ± 0.08 and 1.36 ± 0.11 vs. 2.61 ± 0.32; caspase-3, 1.10 ± 0.05 and 1.94 ± 0.04 vs. 1.40 ± 0.07; Bcl-2, 2.84 ± 0.09 and 2.78 ± 0.14 vs. 0.38 ±

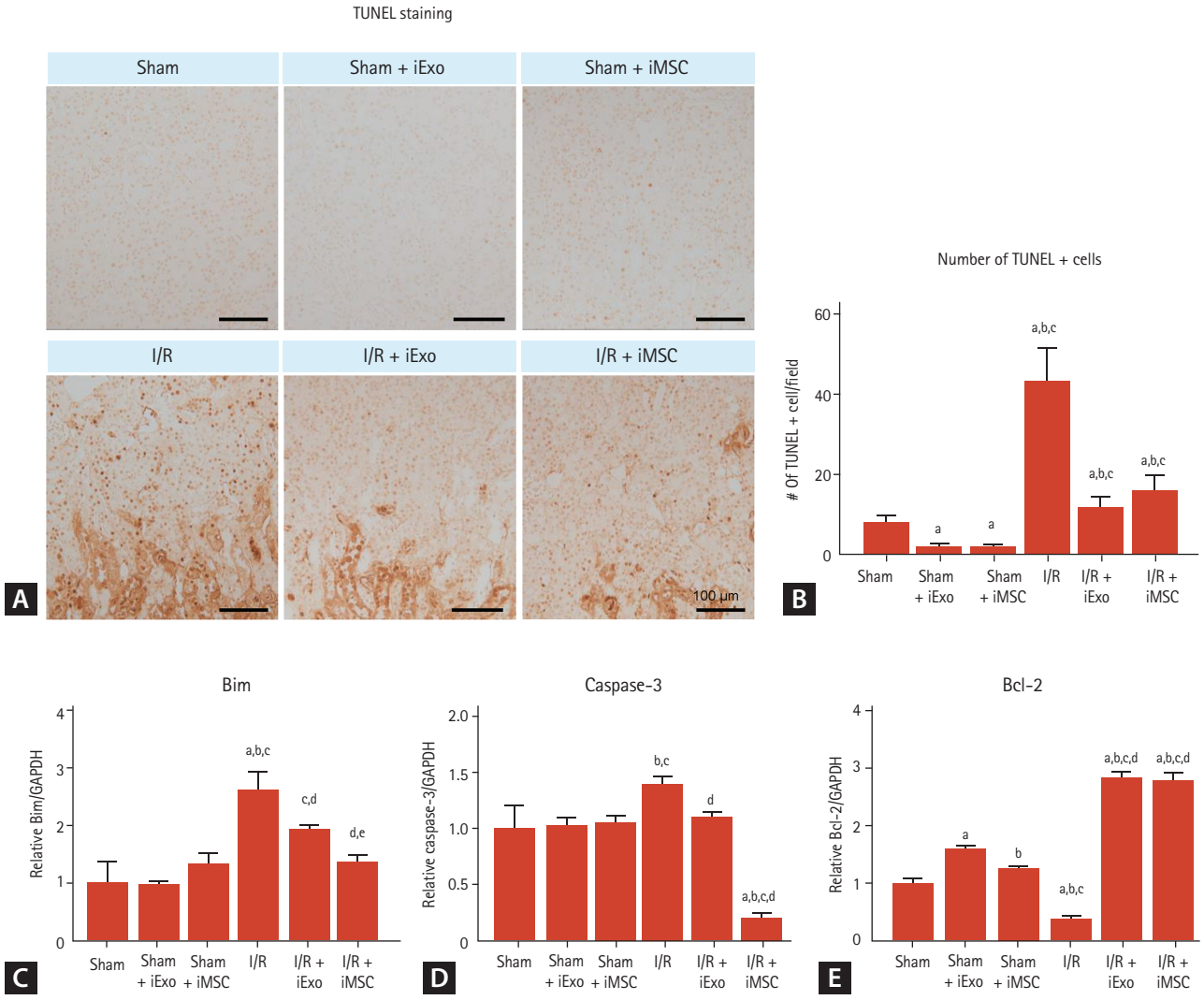

Figure 3. Effects of treatment with mesenchymal stem cells (iMSCs) or iMSC-derived exosome (iExo) on apoptosis in renal ischemia reperfusion (I/R) injury mouse model. (A) Representative images of *in situ* terminal deoxynucleotidyl transferase dUTP nick end labeling (TUNEL) staining. (B) Quantification of TUNEL-positive cells. Quantitative real-time polymerase chain reaction analysis of (C) Bim, (D) caspase-3, and (E) B-cell lymphoma 2 (Bcl-2) levels in kidney tissues. All results are representative of at least three independent experiments. Data are presented as mean ± standard error. Scale bar = 100 μm. [a]$p < 0.05$ vs. Sham, [b]$p < 0.05$ vs. Sham + iMSC, [c]$p < 0.05$ vs. Sham + iExo, [d]$p < 0.05$ vs. I/R, [e]$p < 0.05$ vs. I/R + iMSC.

0.05, $p < 0.05$ vs. the I/R group) (Fig. 3C-3E). The I/R + iMSC group demonstrated decreased Bim and caspase-3 mRNA levels compared to the I/R + iExo group.

Effects of treatment with iExo or iMSCs on oxidative stress induced by renal I/R injury

I/R injury induced significantly increased urinary 8-OHdG excretion, an indicator of oxidative DNA damage in urine and kidney tissues, compared to the sham group (9.95 ± 1.2 vs. 1.41 ± 0.4, $p < 0.05$ vs. the sham group) (Fig. 4). However, this level was significantly decreased after treatment with iExo and iMSC (4.92 ± 0.4 and 7.35 ± 1.0, $p < 0.05$ vs. the I/R group). Abundant nuclear 8-OHdG immunoreactivity in kidney tissues from the I/R group was also attenuated in the I/R + iExo and I/R + iMSC groups (Fig. 4B). Fig. 5C illustrates the significantly decreased renal 8-OHdG staining after iExo and iMSC treatment during I/R (11.10 ± 0.7 and 18.57 ± 2.5 vs. 36.50 ± 5.4, $p < 0.05$ vs. the I/R group).

https://doi.org/10.3904/kjim.2020.438

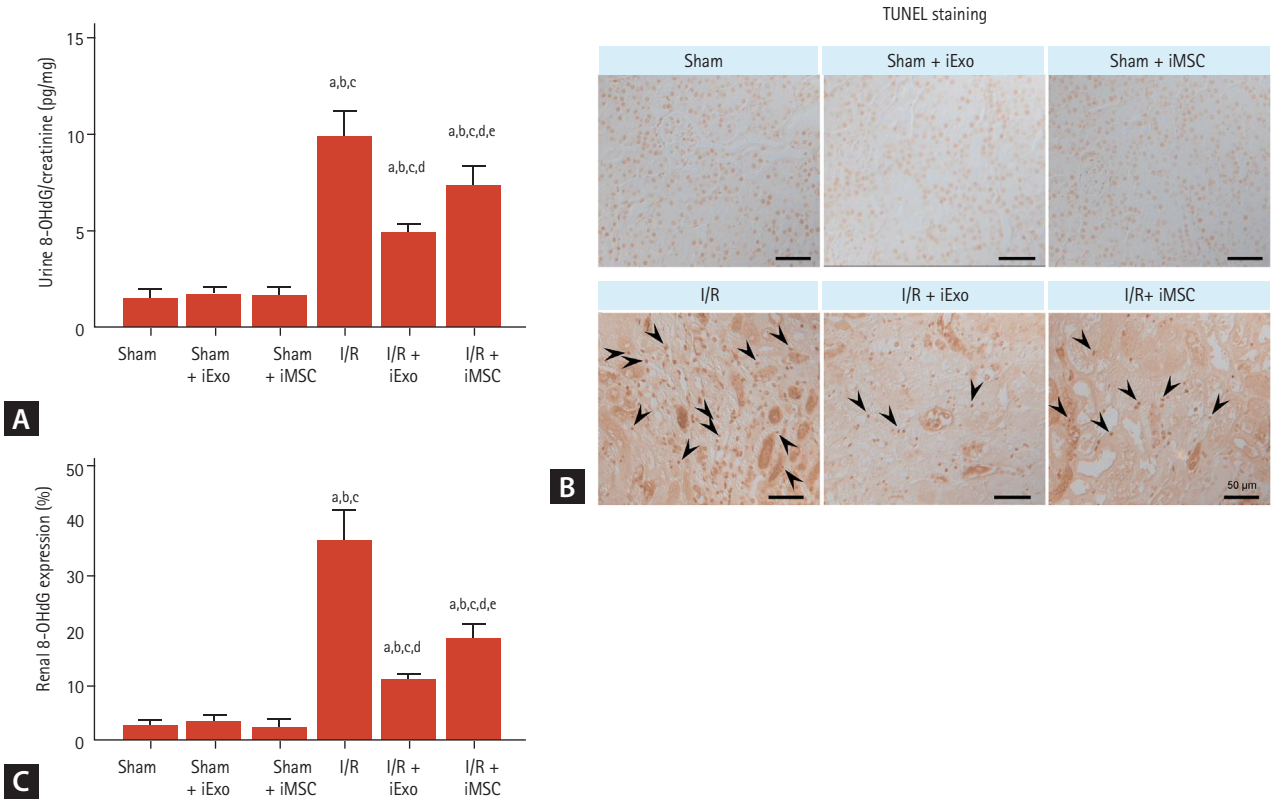

Figure 4. Effects of treatment with mesenchymal stem cells (iMSCs) or iMSC-derived exosome (iExo) on the expression of 8-hydroxy-2′-deoxyguanosine (8-OHdG). (A) 8-OHdG level in urine. (B, C) Representative image and quantification of immunostaining of 8-OHdG in kidney tissues. Arrow heads indicate 8-OHdG-positive cells. Data are presented as mean ± standard error. Scale bar = 50 μm. I/R, ischemia reperfusion. [a]p < 0.05 vs. Sham, [b]p < 0.05 vs. Sham+iMSC, [c]p < 0.05 vs. Sham + iExo, [d]p < 0.05 vs. I/R, [e]p < 0.05 vs. I/R + iMSC.

Effect of iExo or iMSC treatment on antioxidant and pro-inflammation gene expression levels

We examined the effect of treatment with iExo and iMSCs on the transcriptional levels of genes associated with antioxidants and pro-inflammation during I/R injury (Fig. 5). As expected, I/R injury significantly decreased mRNA levels of SOD2, catalase, and NRF2, which are associated with antioxidants (SOD, 0.65 ± 0.1 vs. 1.0 ± 0.1; catalase, 0.18 ± 0.01 vs. 1.0 ± 0.1, NRF2, 0.58 ± 0.1 vs. 1.0 ± 0.2, $p < 0.05$ vs. the sham group). However, treatment with iExo and iMSCs significantly restored these levels, as shown in Fig. 5A-5C (SOD, 1.15 ± 0.2 and 1.55 ± 0.1; catalase, 11.10 ± 0.7 and 18.57 ± 2.5; NRF2, 1.17 ± 0.1 and 0.99 ± 0.1, P < 0.05 vs. the I/R group). Consistent with these results, mRNA levels of NF-κB, TNFα, IFNγ, and IL-1β during I/R injury were also significantly attenuated by treatment with iExo or iMSC (NF-κB, 1.77 ± 0.2 and 1.06 ± 0.3 vs. 2.70 ± 0.1; TNFα, 1.87 ± 0.3 and 1.0 ± 0.7 vs. 3.20 ± 0.3; IFNγ, 1.46 ± 0.1 and 0.41 ± 0.1 vs. 1.71 ± 0.1; IL-1β, 1.25 ± 0.1 and 1.22 ± 0.2 vs. 2.47 ± 0.1, $p < 0.05$ vs. the I/R group).

Effects of iExo or iMSC treatment on ERK1/2 signaling pathway activation

Next, we evaluated whether the protective effects of iExo and iMSCs were associated with the signaling cascade of the extracellular signal-regulated kinase (ERK) signaling pathway, which plays an important role in cell death and survival during renal I/R injury. Activation of ERK1/2 signaling cascades was examined using immunoblot analysis based on the relative amounts of p-MEK1/2 and p-ERK1/2 (Fig. 6). Renal I/R for 25 minutes significantly decreased the ratios of both p-MEK1/2 to total-MEK1/2 (t-MEK1/2) and p-ERK1/2 to t-ERK1/2 (p-MEK1/2/t-MER1/2, 49 ± 2 vs. 100 ± 4; p-ERK1/2/t-ERK1/2, 51 ± 4 vs. 100 ± 5, $p < 0.05$ vs. the sham group). However, iExo or iMSC treatment significantly

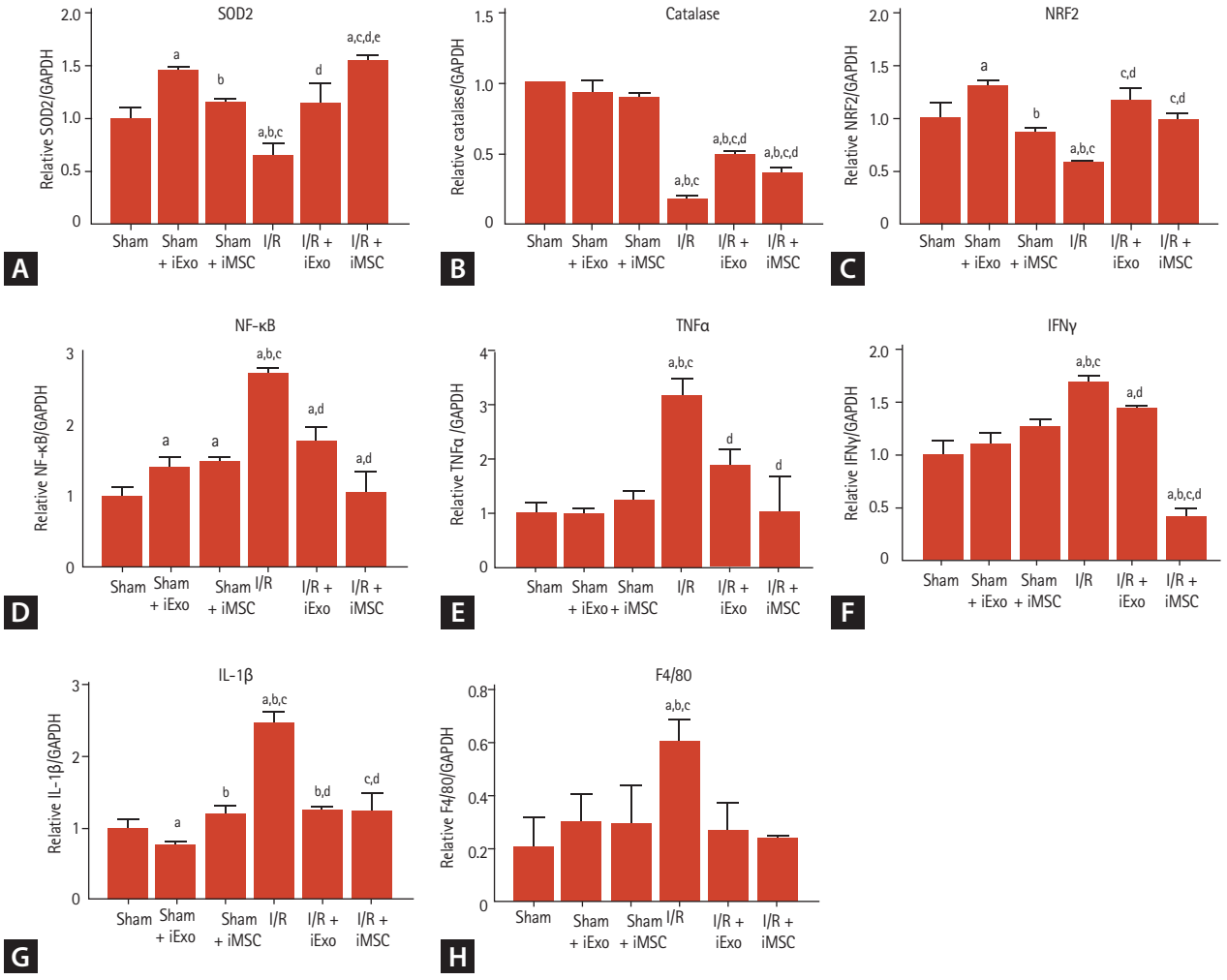

Figure 5. Effects of treatment with mesenchymal stem cells (iMSCs) or iMSC-derived exosome (iExo) on the mRNA levels of antioxidant and inflammatory genes in renal ischemia reperfusion (I/R) injury mouse model. Quantitative real-time polymerase chain reaction analysis of (A) superoxide dismutase 2 (SOD2), (B) catalase, (C) nuclear factor erythroid-2-related factor (NRF2), (D) nuclear factor κB (NF-κB), (E) tumor necrosis factor-α (TNFα), (F) interferon γ (IFNγ), (G) interleukin 1β (IL-1β), and (H) F4/80 expression in kidney tissues. All results are representative of at least three independent experiments. Data are presented as mean ± standard error. GAPDH, glyceraldehyde 3-phosphate dehydrogenase. [a]$p < 0.05$ vs. Sham, [b]$p < 0.05$ vs. Sham + iMSC, [c]$p < 0.05$ vs. Sham + iExo, [d]$p < 0.05$ vs. I/R, [e]$p < 0.05$ vs. I/R + iMSC.

restored these levels (p-MEK1/2/t-MER1/2, 81 ± 2 and 73 ± 4; p-ERK1/2/t-ERK1/2, 81 ± 5 and 84 ± 4, $p < 0.05$ vs. the I/R group), as shown in Fig. 6. Protein expression between the I/R + iExo and I/R + iMSC groups did not differ significantly.

DISCUSSION

The results of the present study demonstrated that iExo administration could reduce renal I/R injury in a mouse model. We found that treatment with iExo attenuated renal dysfunction and the histological changes accompanying reduced inflammation, oxidative stress, and apoptosis. In addition, activation of the ERK1/2 phosphorylation signaling pathway was increased after iExo treatment during I/R injury. Therefore, we suggest that treatment with iExo effectively ameliorates renal damage following I/R injury by enhancing the cell growth and survival signaling pathway.

Many studies have shown that exosomes derived from BMSCs can alleviate tissue damage and promote functional recovery after ischemic injury [17,19]. Because iMSCs have been demonstrated to have a strong therapeutic function,

https://doi.org/10.3904/kjim.2020.438

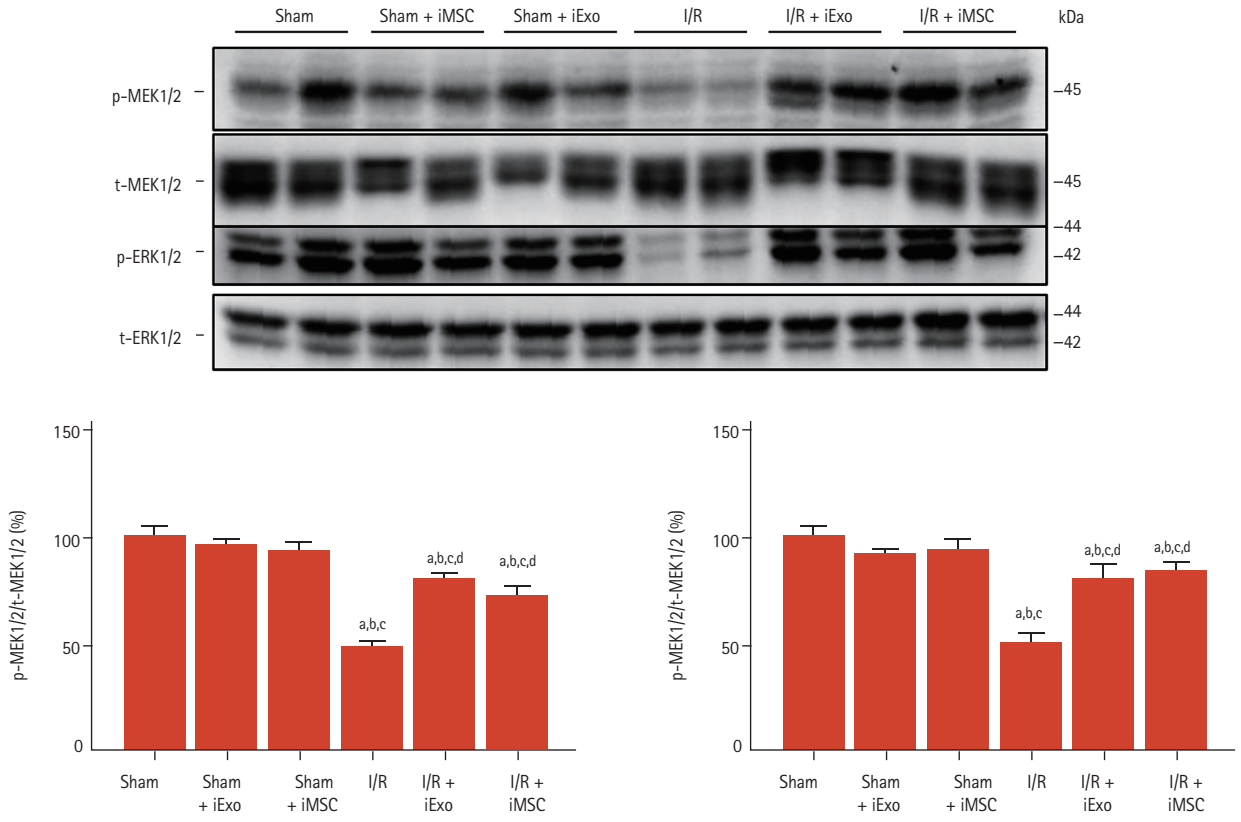

Figure 6. Effect of treatment with mesenchymal stem cells (iMSCs) or iMSC-derived exosome (iExo) on the expression of the extracellular-signal-regulated kinase 1/2 (ERK1/2) signaling pathway in renal ischemia reperfusion (I/R) injury mouse model. (A) Representative immunoblot images and quantification of (B) phosphorylated-mitogen-activated protein kinase kinase 1/2 (p-MEK1/2) and (C) p-ERK1/2 in the kidney tissues. Data are presented as mean ± standard error. t-, total. [a]$p < 0.05$ vs. Sham, [b]$p < 0.05$ vs. Sham + iMSC, [c]$p < 0.05$ vs. Sham + iExo, [d]$p < 0.05$ vs. I/R.

we proposed that iMSC-derived exosomes may also exert powerful attenuating effects on I/R injuries. Therefore, we performed *in vivo* experiments using an I/R mouse model to prove our hypothesis. Consistent with our hypothesis, mice in the iExo-treated group exhibited lower sCr levels and ATN scores than those in the I/R group. Further, treatment with iExo reduced the expression of inflammatory cytokines and markers for oxidative stress and apoptosis. These data confirmed that iExo was functionally active and effective in reducing kidney damage induced by I/R.

ERK1/2 is required to repair renal tubular epithelial cells and inhibit fibrosis caused by renal injury [25], suggesting that the ERK1/2 signaling pathway is related to the pathophysiology of various renal diseases, including renal I/R [26]. In a recent study, the injection of exosomes from human-bone-marrow-derived MSC (hBMSC-Exos) into mice suffering from I/R injury resulted in improved functional recovery, histologic protection, and reduced apoptotic cell death [27]. For direct evidence, they treated human kidney 2 (HK-2) cells exposed to hypoxia/reoxygenation with hBMSC-Exos and found significantly reduced apoptosis accompanied by activation of the ERK signaling pathway in the HK-2 cells compared to the controls [27]. In this study, the I/R injury group demonstrated significant inactivation of the ERK signaling pathway with decreased p-MEK1/2 and p-ERK1/2 levels in kidney tissues compared to the sham group. However, iExo treatment significantly restored these levels, demonstrating similar results as in the iMSC treatment group. Although not explainable in this study, the exosome-enriched fraction has been reported to exhibit the highest renal protection activity from injury [28]. ERK1/2 signaling was shown to be activated in human dermal fibroblasts following treatment with exosomes collected from the culture supernatant of BMSCs [29]. Taken together, our

results suggest that iExo treatment protects against I/R-induced renal injury, in which the ERK1/2 signaling pathway played an important role.

The efficacy of many MSC-based therapies has been attributed to the paracrine secretion of trophic factors, and exosomes may play a major role in mediating tissue repair [30,31]. Exosomes derived from different stem cells, such as BMSCs and adipose-derived MSCs, have been shown to attenuate injury [32-36]. In the present study, we selected exosomes derived iMSC (iExo) to treat renal I/R injury for several reasons. First, the effect of iPSC-derived MSC exosomes on renal IR injury has not been investigated. Second, iPSCs can generate unlimited amounts of early passage MSC with consistent quality. Third, iExo are a promising cell source for autologous cell therapies in regenerative medicine. Fourth, compared to adult MSCs, human iMSCs have been demonstrated to be superior regarding cell proliferation, immunomodulation, cytokine profile, generation of exosomes capable of modulating the microenvironment, and bioactive paracrine factor secretion [9,10,37].

Several studies have examined *in vivo* tracking to determine exosome biodistribution upon systemic delivery [38,39]. In an AKI mouse model, intravenously injected DiD-labeled extracellular vesicles (EVs), including exosomes, accumulated predominantly in the kidney of mice with AKI compared to healthy control [40]. Eventually, exosomes internalized by renal epithelial cell membrane fusion or endocytosis play a protective role in kidney injury and promote tissue regeneration and repair [41]. Until now, it is unclear how long exosomes exist in kidney lesions. However, several studies showed that exosomes have a short half-life *in vivo* [42,43], limiting their therapeutic potential for clinical application. Various forms of hydrogels such as chitosan/silk hydrogel, chitosan hydrogel, and imine crosslinking hydrogel have been used to enhance the therapeutic effects of exosomes [44-47]. Finally, secreted EVs can be eliminated as cellular waste. This might be a more efficient strategy for eliminating senescent proteins compared to proteasomal and lysosomal degradation [48].

Our study had several limitations. First, although the present study results are promising, the study period was only 24 hours; the long-term effects of iExo therapy for I/R injury remain uncertain. Second, although we systemically injected iExo via the tail vein, we only focused on its effects on the kidneys and not on other organs. Third, we did not observe a direct role of iExo *in vitro* to help elucidate its protective mechanism. Future studies are warranted to define the exact role of iExo in hypoxia-related conditions.

In conclusion, the present study demonstrated that exosomes from iPSC-derived MSC therapy effectively preserve renal function and the integrity of the kidney against I/R injury. These findings suggest a potential therapeutic approach for various types of AKI.

KEY MESSAGE

1. Mesenchymal stem cells (iMSC)-derived exosomes ameliorate renal dysfunction and the histological changes accompanying reduced inflammation, oxidative stress, and apoptosis following ischemia reperfusion injury in a mouse model.
2. iMSC-derived exosomes protect against ischemia reperfusion-induced renal injury, in which the extracellular signal-regulated kinase (ERK) 1/2 signaling pathway plays an important role.
3. Our findings suggest that iMSC-derived exosomes are useful for autologous treatment with unlimited amounts of iMSC. Also, the safety issue of cell-based therapy can be excluded.

Conflict of interest

Kyung Woon Kim is an employee of OncoInsight Co. Ltd., but no potential conflict of interest relevant to this article was reported.

Acknowledgments

This work was supported by the Korean Health Technology R&D Project, Ministry for Health & Welfare, Republic of Korea (HI14C3417), and the Basic Science Research Program through the National Research Foundation of Korea (NRF) funded by the Ministry of Science, ICT & Future Planning (NRF-2018R1D1A1A02043014).

REFERENCES

1. Basile DP, Anderson MD, Sutton TA. Pathophysiology of acute kidney injury. Compr Physiol 2012;2:1303-1353.
2. Vinas JL, Burger D, Zimpelmann J, et al. Transfer of microRNA-486-5p from human endothelial colony forming cell-derived exosomes reduces ischemic kidney injury. Kidney Int

https://doi.org/10.3904/kjim.2020.438

2016;90:1238-1250.
3. Han SJ, Lee HT. Mechanisms and therapeutic targets of ischemic acute kidney injury. Kidney Res Clin Pract 2019;38:427-440.
4. Rosner MH, Perazella MA. Acute kidney injury in the patient with cancer. Kidney Res Clin Pract 2019;38:295-308.
5. Cecka M. Clinical outcome of renal transplantation. Factors influencing patient and graft survival. Surg Clin North Am 1998;78:133-148.
6. Godwin JG, Ge X, Stephan K, Jurisch A, Tullius SG, Iacomini J. Identification of a microRNA signature of renal ischemia reperfusion injury. Proc Natl Acad Sci U S A 2010;107:14339-14344.
7. Tilney NL, Guttmann RD. Effects of initial ischemia/reperfusion injury on the transplanted kidney. Transplantation 1997;64:945-47.
8. Hirschi KK, Li S, Roy K. Induced pluripotent stem cells for regenerative medicine. Annu Rev Biomed Eng 2014;16:277-294.
9. Diederichs S, Tuan RS. Functional comparison of human-induced pluripotent stem cell-derived mesenchymal cells and bone marrow-derived mesenchymal stromal cells from the same donor. Stem Cells Dev 2014;23:1594-1610.
10. Lian Q, Zhang Y, Zhang J, et al. Functional mesenchymal stem cells derived from human induced pluripotent stem cells attenuate limb ischemia in mice. Circulation 2010;121:1113-1123.
11. Rubio D, Garcia S, Paz MF, et al. Molecular characterization of spontaneous mesenchymal stem cell transformation. PLoS One 2008;3:e1398.
12. Jeong JO, Han JW, Kim JM, et al. Malignant tumor formation after transplantation of short-term cultured bone marrow mesenchymal stem cells in experimental myocardial infarction and diabetic neuropathy. Circ Res 2011;108:1340-1347.
13. Ratajczak MZ, Suszynska M, Borkowska S, Ratajczak J, Schneider G. The role of sphingosine-1 phosphate and ceramide-1 phosphate in trafficking of normal stem cells and cancer cells. Expert Opin Ther Targets 2014;18:95-107.
14. Thery C, Zitvogel L, Amigorena S. Exosomes: composition, biogenesis and function. Nat Rev Immunol 2002;2:569-579.
15. Kwon SH. Extracellular vesicles in renal physiology and clinical applications for renal disease. Korean J Intern Med 2019;34:470-479.
16. Record M, Carayon K, Poirot M, Silvente-Poirot S. Exosomes as new vesicular lipid transporters involved in cell-cell communication and various pathophysiologies. Biochim Biophys Acta 2014;1841:108-120.
17. Arslan F, Lai RC, Smeets MB, et al. Mesenchymal stem cell-derived exosomes increase ATP levels, decrease oxidative stress and activate PI3K/Akt pathway to enhance myocardial viability and prevent adverse remodeling after myocardial ischemia/reperfusion injury. Stem Cell Res 2013;10:301-312.
18. Bian S, Zhang L, Duan L, Wang X, Min Y, Yu H. Extracellular vesicles derived from human bone marrow mesenchymal stem cells promote angiogenesis in a rat myocardial infarction model. J Mol Med (Berl) 2014;92:387-397.
19. Xin H, Chopp M, Shen LH, et al. Multipotent mesenchymal stromal cells decrease transforming growth factor β1 expression in microglia/macrophages and down-regulate plasminogen activator inhibitor 1 expression in astrocytes after stroke. Neurosci Lett 2013;542:81-86.
20. Lai RC, Yeo RW, Tan KH, Lim SK. Mesenchymal stem cell exosome ameliorates reperfusion injury through proteomic complementation. Regen Med 2013;8:197-209.
21. Kosaka N, Yoshioka Y, Hagiwara K, Tominaga N, Ochiya T. Functional analysis of exosomal microRNA in cell-cell communication research. Methods Mol Biol 2013;1024:1-10.
22. Shin YJ, Luo K, Quan Y, et al. Therapeutic challenge of minicircle vector encoding klotho in animal model. Am J Nephrol 2019;49:413-424.
23. Lien YH, Yong KC, Cho C, Igarashi S, Lai LW. S1P(1)-selective agonist, SEW2871, ameliorates ischemic acute renal failure. Kidney Int 2006;69:1601-1608.
24. Lim SW, Shin YJ, Luo K, et al. Ginseng increases Klotho expression by FoxO3-mediated manganese superoxide dismutase in a mouse model of tacrolimus-induced renal injury. Aging (Albany NY) 2019;11:5548-5569.
25. Jang HS, Han SJ, Kim JI, Lee S, Lipschutz JH, Park KM. Activation of ERK accelerates repair of renal tubular epithelial cells, whereas it inhibits progression of fibrosis following ischemia/reperfusion injury. Biochim Biophys Acta 2013;1832:1998-2008.
26. Kumar S, Allen DA, Kieswich JE, et al. Dexamethasone ameliorates renal ischemia-reperfusion injury. J Am Soc Nephrol 2009;20:2412-2425.
27. Zhu G, Pei L, Lin F, et al. Exosomes from human-bone-marrow-derived mesenchymal stem cells protect against renal ischemia/reperfusion injury via transferring miR-199a-3p. J Cell Physiol 2019;234:23736-23749.
28. Collino F, Pomatto M, Bruno S, et al. Exosome and microvesicle-enriched fractions isolated from mesenchymal stem cells by gradient separation showed different molecular signatures

and functions on renal tubular epithelial cells. Stem Cell Rev Rep 2017;13:226-243.
29. Shabbir A, Cox A, Rodriguez-Menocal L, Salgado M, Van Badiavas E. Mesenchymal stem cell exosomes induce proliferation and migration of normal and chronic wound fibroblasts, and enhance angiogenesis in vitro. Stem Cells Dev 2015;24:1635-1647.
30. Liang X, Ding Y, Zhang Y, Tse HF, Lian Q. Paracrine mechanisms of mesenchymal stem cell-based therapy: current status and perspectives. Cell Transplant 2014;23:1045-1059.
31. Baglio SR, Pegtel DM, Baldini N. Mesenchymal stem cell secreted vesicles provide novel opportunities in (stem) cell-free therapy. Front Physiol 2012;3:359.
32. Orozco L, Munar A, Soler R, et al. Treatment of knee osteoarthritis with autologous mesenchymal stem cells: a pilot study. Transplantation 2013;95:1535-1541.
33. Wakitani S, Yamamoto T. Response of the donor and recipient cells in mesenchymal cell transplantation to cartilage defect. Microsc Res Tech 2002;58:14-18.
34. Chiang ER, Ma HL, Wang JP, Liu CL, Chen TH, Hung SC. Allogeneic mesenchymal stem cells in combination with hyaluronic acid for the treatment of osteoarthritis in rabbits. PLoS One 2016;11:e0149835.
35. ter Huurne M, Schelbergen R, Blattes R, et al. Antiinflammatory and chondroprotective effects of intraarticular injection of adipose-derived stem cells in experimental osteoarthritis. Arthritis Rheum 2012;64:3604-3613.
36. Koh YG, Choi YJ, Kwon SK, Kim YS, Yeo JE. Clinical results and second-look arthroscopic findings after treatment with adipose-derived stem cells for knee osteoarthritis. Knee Surg Sports Traumatol Arthrosc 2015;23:1308-1316.
37. Sabapathy V, Kumar S. hiPSC-derived iMSCs: NextGen MSCs as an advanced therapeutically active cell resource for regenerative medicine. J Cell Mol Med 2016;20:1571-1588.
38. Wiklander OP, Nordin JZ, O'Loughlin A, et al. Extracellular vesicle in vivo biodistribution is determined by cell source, route of administration and targeting. J Extracell Vesicles 2015;4:26316.
39. Choi H, Lee DS. Illuminating the physiology of extracellular vesicles. Stem Cell Res Ther 2016;7:55.
40. Grange C, Tapparo M, Bruno S, et al. Biodistribution of mesenchymal stem cell-derived extracellular vesicles in a model of acute kidney injury monitored by optical imaging. Int J Mol Med 2014;33:1055-1063.
41. Wang R, Lin M, Li L, et al. Bone marrow mesenchymal stem cell-derived exosome protects kidney against ischemia reperfusion injury in rats. Zhonghua Yi Xue Za Zhi 2014;94:3298-3303.
42. Imai T, Takahashi Y, Nishikawa M, et al. Macrophage-dependent clearance of systemically administered B16BL6-derived exosomes from the blood circulation in mice. J Extracell Vesicles 2015;4:26238.
43. Takahashi Y, Nishikawa M, Shinotsuka H, et al. Visualization and in vivo tracking of the exosomes of murine melanoma B16-BL6 cells in mice after intravenous injection. J Biotechnol 2013;165:77-84.
44. Liu X, Yang Y, Li Y, et al. Integration of stem cell-derived exosomes with in situ hydrogel glue as a promising tissue patch for articular cartilage regeneration. Nanoscale 2017;9:4430-4438.
45. Pape AC, Bakker MH, Tseng CC, et al. An injectable and drug-loaded supramolecular hydrogel for local catheter injection into the pig heart. J Vis Exp 2015;100:e52450.
46. Xu L, Yu JQ, Wang XY, Xu N, Liu JL. Microwave extraction optimization using the response surface methodology of Fructus Meliae Toosendan polysaccharides and its antioxidant activity. Int J Biol Macromol 2018;118(Pt B):1501-1510.
47. Zhang K, Zhao X, Chen X, et al. Enhanced therapeutic effects of mesenchymal stem cell-derived exosomes with an injectable hydrogel for hindlimb ischemia treatment. ACS Appl Mater Interfaces 2018;10:30081-30091.
48. van Balkom BW, Pisitkun T, Verhaar MC, Knepper MA. Exosomes and the kidney: prospects for diagnosis and therapy of renal diseases. Kidney Int 2011;80:1138-1145.

https://doi.org/10.3904/kjim.2020.438